Conf-950801--5

SAN095-1292C

Guest-Host Crosslinked Polyimides for Integrated Optics

T.C. Kowalczyk, T.Z Kosc, and K.D. Singer
Case Western Reserve University, Department of Physics, Cleveland, OH 44106-7079

A.J. Beuhler* and D.A. Wargowski
Amoco Research Center, Amoco Chemical Co., Naperville, IL 60566
** Present Address: Motorola Corp., Northbrook, IL 60062*

P.A. Cahill, C.H. Seager, and M.B. Meinhardt
Sandia National Laboratories, Division 1811, Albuquerque, NM 87185-1407

We report on the optical and electrical characterization of aromatic, fluorinated, fully imidized, organic soluble, thermally and photochemically crosslinkable, guest-host polyimides for integrated optics. Refractive indices and optical losses were measured to evaluate the performance of these materials for passive applications. Materials were doped with two high temperature nonlinear optical chromophores, and poled during crosslinking to produce nonlinear optical materials. Measurements of electro-optic coefficient, macroscopic second order susceptibility, and conductivity were performed to assess these materials as potential candidates for active devices.

High speed optical interconnects and switches are being investigated to eliminate the optical-to-electrical signal bottleneck in high speed communication and data transfer. Recent efforts have concentrated on developing new optimized materials for integrated optics. Organic polymers have received much attention as potential candidates and are promising materials for integrated optics because they have low optical losses, low dielectric constants, and are compatible with existing silicon fabrication procedures.[1] Furthermore, polymers can be cast into multiple layer structures containing channels, ribs, and other routing structures. The ability to define multiple layer structures allows high densities of optical interconnects and facilitates high speed signal routing and multiplexing.

The successful incorporation of active polymeric materials into integrated optics depends on the degree to which the following parameters can be simultaneously optimized: optical loss, waveguide formation, optical nonlinearity, and thermal stability. This optimization will likely be based on a series of trade-offs. For example, large nonlinearities can be obtained by operating near resonance with a large chromophore concentration at the cost of severe optical absorption. The first two parameters, optical loss and waveguide formation, characterize the ability of these materials to serve as passive optical interconnects. Since low optical losses in polymers are achievable, a natural step in the development of nonlinear optical polymers is to convert low optical loss polymers into nonlinear optical materials by mixing chromophores with large nonlinearities ($\mu\beta$ products) into the polymer matrix and inducing noncentrosymmetric ordering by electric field poling. However, the ordering induced by poling places the polymer in a state of non-equilibrium leading to time and temperature dependent decay of the optical nonlinearity. Initial nonlinear optical hosts such as

DISTRIBUTION OF THIS DOCUMENT IS UNLIMITED
DISTRIBUTION OF THIS DOCUMENT IS UNLIMITED

MASTER

DISCLAIMER

This report was prepared as an account of work sponsored by an agency of the United States Government. Neither the United States Government nor any agency thereof, nor any of their employees, make any warranty, express or implied, or assumes any legal liability or responsibility for the accuracy, completeness, or usefulness of any information, apparatus, product, or process disclosed, or represents that its use would not infringe privately owned rights. Reference herein to any specific commercial product, process, or service by trade name, trademark, manufacturer, or otherwise does not necessarily constitute or imply its endorsement, recommendation, or favoring by the United States Government or any agency thereof. The views and opinions of authors expressed herein do not necessarily state or reflect those of the United States Government or any agency thereof.

DISCLAIMER

Portions of this document may be illegible in electronic image products. Images are produced from the best available original document.

polymethylmethacrylate, polystyrene and polycarbonate have low optical loss, but also low glass transition temperatures, which leads to rapid decay of poling induced orientation at near ambient temperatures. The nonlinearity of these materials is limited because increased dopant loading causes aggregation and plasticization.

Further attempts to optimize the $\mu\beta$ product and thermal stability included the use of main chain chromophores, side chain chromophores, and crosslinked systems.[2–4] These materials have higher glass transition temperatures and reduced mobility as compared to their guest-host analogs and consequently reduced chromophore relaxation. Guest-host polyimides have been employed to optimize thermal stability of induced orientation while maintaining functionality. Polyimides are well known in the electronics industry for their thermal integrity, resistance to organic solvents, and compatibility with silicon fabrication processes. Initial guest-host polyimides required imidization and densification at temperatures greater than 300° C to retain their induced ordering while exposed to a 200°C environment.[5,6] The high processing temperature of these materials requires dopant molecules to have high thermal decomposition temperatures. In studies where the chromophores did not thermally decompose, sublimation and plasticization occurred.[7,8] Alternatives to high temperature imidization have been developed and include chemical imidization and preimidized soluble polyimides.[9,10] In these cases, densification for extended periods of time was necessary to minimize the free volume around the chromophore and reduce thermal relaxation of induced orientation.[11] More recently, side-chain polyimides have been developed.[12–14] These materials imidize at temperatures below the thermal decomposition temperatures of most chromophores and have demonstrated excellent thermal stability of induced orientation for over 200 hours at elevated temperatures . The additional orientational stability is presumably due to the hindered rotational motion of the large polyimide chains. The optical losses and processability of these materials remain unreported.

In this chapter, we report on our approach to the development of device-quality electro-optic materials. We have sought to optimize the optical losses and processing properties first, and later to functionalize the materials having learned how to synthesize and process them for devices. We started with perfluorinated preimidized fully aromatic polyimides. Preimidization makes processing doped polymer systems more flexible, by making functionalizing easier while allowing spin coating of soluble fully-imidized polymers. Fluorination increases solubility while decreasing optical loss and refractive index. Fully aromatic polymers allow for the best high temperature properties. We found that by introducing alkylated aromatic crosslinking groups which can be photo- or thermally activated, optical losses were greatly reduced, and high quality waveguides could be fabricated. Another advantage of the crosslinking groups is that they open up new processing capabilities. For example, crosslinking allows simple multilayer formation, since the crosslinked polymers do not dissolve when subsequent layers are spin deposited. The photo-crosslinking also permits a simple liquid etch process to define waveguides, and provides a chemical hook to which chromophores may be covalently attached to these polymers. After optimizing the loss and processing using this crosslinking chemistry, we studied the functionalization of these polymers using poled guest chromophores. We have uncovered a number of issues relating to functionalization, such as increased optical loss due to long absorption tails in the chromophore and enhanced mobility of small chromophores. We have also studied poling issues related to multilayer films. We believe that our approach for material development, focused on the processing

and operation of devices, has led to a flexible material system with exceptional promise for the development of electro-optic polymer devices.

1. Polymer Waveguides

We studied optical losses in polyimide waveguides in order to understand the mechanisms responsible for losses and to develop new polyimides with lower losses. Waveguide losses are caused by absorption and scattering which can be either extrinsic or intrinsic.[15] Intrinsic absorption at long wavelengths is due to (C-H) carbon-hydrogen bond combination and overtone bands, and at short wavelengths, from electronic absorptions. Extrinsic absorption and scattering are caused by waveguide nonuniformities and contaminants in the polymer. The first polyimide synthesized for optical applications, PMDA-ODA (Pyromellitic dianhydride oxydianiline),had high losses.[16] Losses were significantly reduced by attaching perfluoro (CF_3) groups to the polymer backbone. The addition of these groups decreased absorption in the visible wavelengths by reducing charge transfer and creating polymer deformation.[17–19] Losses were cure dependent. Scattering losses, which are attributed to waveguide refractive index fluctuations, are also dependent on cure and structure. The inability to separate scattering and absorptive losses has limited the development of optical polyimides.

The most direct method to measure absorption is UV-visible spectroscopy. Unfortunately, UV-visible spectroscopy is not sensitive at the level of 1 dB/cm in thin film transmission measurements. Uncertainties in material properties lead to large errors in absorption coefficients calculated from absorption spectra.[20] More sensitive absorption techniques such as photothermal deflection spectroscopy (PDS) have been used to measure pure absorptive losses in polymers.[21] Using PDS along with waveguide loss spectroscopy (WLS), which measures the sum of scattering and absorption losses, the mechanisms of optical loss can be isolated.

Waveguide losses were measured using the scattered streak method. Measurements were made by coupling polarized light into the lowest order guided mode and capturing a video image of the guided streak with a CCD camera. This method assumes that the intensity of guided light is proportional to the intensity of scattered light. The digitized image was converted to an intensity vs distance plot from which the optical loss was determined. The sensitivity of WLS allows losses between 0.3 and 50 dB/cm to be measured. Losses greater than 50 dB/cm produce a guided streak too short to be measured accurately, and losses lower than 0.3 dB/cm do not scatter enough light out of the waveguide.

The PDS measurements were carried out in the transverse mode using a highly stable, single mode, 632 nm He-Ne laser.[22] The heating beam was provided by a 19 Hz chopped beam from a short arc, high pressure Xenon lamp passing through a single pass grating monochrometer with a band pass of 12 nm. A partially masked Si photo-cell served as the probe beam detector, while the heating beam intensity was continuously monitored with a second Si photo-cell for normalization purposes. Spectrum normalization was accomplished by comparing the sample PDS response with that obtained with a reference sample fabricated by baking a flat black organic coating of low reflectivity (4%) on quartz substrates. Independent measurements of the reflectivity of this calibration standard were made by routine methods. With proper vibration isolation of the PDS apparatus, the noise level for absorbance was 3 ppm. Flourinert FC-75 was chosen as the deflection medium. In the data

reduction it was assumed that the reflectivity of the polymers in FC-75 was not a function of photon energy. Because the optical indices of these polymers did not differ greatly from FC-75, the reflectivity at the polymer/liquid interface was small, and variations of this quantity with photon energy will not introduce serious errors in the calculation of the absorption coefficient. Sample thicknesses were measured with a Sloan Dektak in several locations in the region heated by the PDS pump beam.

Polyimides were synthesized with increasing amounts of fluorination as shown in Fig. 1 (in order of increasing fluorination). The details of synthesis have been reported elsewhere.[23] Refractive indices in Fig. 2 were measured at 632 nm using TM and TE polarized He-Ne laser light. Several trends are apparent from the refractive index data. First, the refractive index and birefringence decrease with increasing fluorination. Decreased refractive indices are attributed to the reduction of conjugation due to twisting of the polymer backbone. The steric hindrance of fluorine-substituted polyimides prevents in-plane packing which decreases the birefringence. The only exception to this trend is Ultradel 9020D, which has a birefringence greater than the unalkylated polyimides. The larger birefringence is a result of its rigid backbone. The low refractive index results from its low density due to the presence of alkylated aromatic crosslinking groups[24] and a high degree of fluorination. Second, birefringence increases with curing temperature for all polyimides due to densification even in highly fluorinated samples. The temperature dependence of optical properties requires that care be taken when processing optical polyimides.

PDS was used to determine the absorption loss in thin polyimide films. Increasing fluorination also decreased absorption as shown in the PDS data of Fig. 3. The decrease in absorption is caused by (CF_3) groups that inhibit charge transfer and interrupt conjugation between electron-deficient imide and electron-rich amine sections. Additional (CF_3) groups were attached to the polymer chain to further increase transparency as well as solubility. The additional fluorines that aid solubility, as in 6FDA/BDAF, also caused the fully imidized material to be susceptible to organic solvents. This problem was overcome by attaching alkylated aromatic crosslinking groups onto the polyimide backbone as in Ultradel 9020D.[24] Crosslinking can be accomplished by photo or thermal methods. The crosslinking polyimide showed the lowest absorptive loss, although it did not have the smallest birefringence. Waveguide losses are shown in Fig. 3 as data points along with PDS spectra(lines). For the polyimides in this study, fluorination reduced the waveguide losses considerably. Fig. 3 contains WLS data that is less than PDS data which is unphysical because WLS measures the sum of absorptive and scattering losses. This discrepancy between PDS and WLS data is a result of slight differences in thermal curing in the different samples used in each measurement as well as experimental uncertainty in both measurement techniques. The cure temperature dependent waveguide losses of Ultradel 9020D are plotted in Fig. 4 from 200^o C to 400^o C. At temperatures greater than 350^o C, increased losses are due to polyimide decomposition. Waveguide loss measurements give information on loss mechanisms including both absorption and scattering. PDS measures the absorption of the material and is not susceptible to scattering effects present in WLS measurements and is more sensitive than ordinary UV-vis spectroscopy. Performing both experiments allows absorption losses and scattering losses to be separated by subtraction. Although both birefringence and absorption decrease with increasing fluorination, the agreement between PDS and WLS data for these polyimides indicates that losses are primarily due to absorption and not scattering.

Active devices must have low optical losses to allow efficient nonlinear interactions to take place over length scales appropriate for integrated optics. Nonlinear optically active devices are made by mixing nonlinear optical chromophores into the host material. The introduction of nonlinear chromophores may introduce additional losses in the form of scattering sites and absorption tails which can be further enhanced upon poling.[25] Fig. 5 depicts the structure of our nonlinear optical dopants, DCM[26,27] and DADC[28]. Fig. 6 shows the PDS spectra for undoped Ultradel 9020D, DCM/Ultradel 9020D, and DADC/Ultradel 9020D at 17% weight fraction. The spectra shows absorptive losses exceeding $\alpha = 11cm^{-1}$ (50.0 dB/cm) at 1.4ev (830nm) for DADC cured at 300° C and absorptive losses of $\alpha = 1.1cm^{-1}$ (5.0 dB/cm) for DCM cured at 175° C. In both cases significant losses are introduced by the chromophore, even at long wavelengths. The additional losses in DADC/Ultradel 9020D at high cure temperatures are attributed to chromophore degradation and possibly phase separation. It is important, then, to develop new chromophores with reduced absorption tails.

2. Electro-Optic Properties

The excellent linear optical properties, preimidized form, and crosslinking nature of Ultradel 9020D make it a suitable candidate for high temperature electro-optic applications.[23,29] Ultradel 9020D was doped with thermally stable chromophores, DCM and DADC, and electric field-poled to impart an electro-optic response. DCM is a highly nonlinear chromophore with low molecular weight that is photo-bleachable in the UV.[26] Using DCM as a dopant, we can obtain large nonlinearities because high number densities are possible. While DCM's decomposition temperature remains above the processing temperature of Ultradel 9020D, other researchers have reported sublimation at temperatures as low as 220° C.[8] DADC, a chromophore developed for high temperature electro-optic applications, has a high nonlinearity, high molecular weight, and is also photo-bleachable in the UV.[28] Using DADC we expect lower nonlinearities than DCM because of lower number densities at a given weight fraction. DADC's larger structure eliminates sublimation even at temperatures as high as 400° C. TGA (thermogravimetric analysis) experiments have shown only a 2% weight loss in nitrogen at temperatures as high as 400° C.[26]

The optimum conditions for poling during crosslinking were investigated. Ideally, the crosslinking reaction and chromophore alignment should proceed simultaneously. Poling at low temperatures can result in reduced alignment because of limited chromophore mobility, while poling the sample at too high temperature limits the ordering due to increased thermal effects and higher conductivity. The optimum poling temperature was determined by comparing samples poled with the same field at varying temperatures. Orientation and relaxation were probed by measuring the in-plane electro-optic coefficient at 800 nm with a Mach-Zehnder interferometer.[30] The electro-optic coefficient was measured immediately after poling for both sets of samples. Afterwards, the samples were placed into an oven at 125° C for approximately 50 hours, and the electro-optic coefficient was remeasured. Table I shows the results for both DADC and DCM. For DADC the electro-optic coefficient before aging is constant with temperature. After thermal aging, the sample poled below 200° C decayed while those above 200° C remained stable. This indicates that crosslinking occurs just above 200° C. The 200° C crosslinking is also observed in dielectric loss measurements as shown in Fig. 7, and in greatly decreased solubility when films are processed at that

temperature.

Table I shows that the ratio, $r_{33}(t)/r_{33}(0)$, for DCM is fairly constant for temperatures above 200° C. At higher temperatures, $r_{33}(0)$ was lower. We attribute this to sublimation of the chromophore at elevated temperatures. Evidence for sublimation is shown in Fig. 8 where a decrease in optical absorption occurred when the doped polymer was processed at 225° C. Interestingly, the chromophore retention depends on the initial concentration which may be evidence of the chromophore plasticizing the polymer. The enhanced orientational decay of DCM at all temperatures may be attributed to plasticizing of the polyimide.[10]

The electric field dependence of the electro-optic coefficient for DADC-doped films is plotted in Fig. 9. Samples were poled using electric fields between 0.1 and 1.3 MV/cm at 200^0 C using a ramp, soak, and cool cycle for a total of 45 minutes. The in-plane electro-optic coefficient was measured as a function of applied field and compared to theoretical calculations using the two level oriented gas model with μ and β obtained from electric field-induced second harmonic generation (EFISH). The equation relating the electro-optic coefficient to its microscopic parameters at a particular wavelength is given by[31],

$$r_{ij,k}(-\omega;\omega,0) = \frac{-4N\beta_{zzz}L_3(p)}{n_\omega^4}\frac{f^\omega f^\omega f^o}{f^{2\omega'}f^{\omega'}f^{\omega'}}\frac{(3\omega_o^2-\omega^2)(\omega_o^2-\omega'^2)(\omega_o^2-4\omega'^2)}{3\omega_o^2(\omega_o^2-\omega^2)^2} \tag{1}$$

$$p = f^o\frac{\mu E_p}{k_B T_p} \tag{2}$$

where N is the chromophore number density, β_{zzz} is the second order microscopic susceptibility, $L_3(p)$ is the third-order Langevin function, μ is the dipole moment, E_p is the poling field, k_B is the Boltzmann constant, T_p is the poling temperature, f^o is the Onsager local field factor for the static poling field, $f^\omega f^{2\omega'} f^{\omega'}$ are the Lorenz-Lorentz local field factors at optical frequencies, ω' and $2\omega'$ are the frequencies used in the second harmonic generation experiment, ω_o and ω are the resonance and electro-optic experiment frequencies, respectively. Fig. 9 shows the agreement between Eq. 1 and experiment indicating full poling and verifies the electronic nature of the electro-optic effect. The solid lines define the $(+/-)15\%$ error in the measurement of $\mu\beta$. The slight offset of electro-optic coefficient at larger poling fields is probably due to increased birefringence with increasing poling fields. Long term thermal stability of induced orientation was measured for DCM- and DADC-doped films. In this experiment, the electro-optic coefficient was measured immediately after poling. Samples were then placed in an oven at 125° C, and samples were retested at subsequent times. The decay of the electro-optic coefficient is shown in Fig. 10. The data show the decay at elevated temperatures for both samples. DCM undergoes a more rapid decay of induced orientation at elevated temperatures indicating that the higher number densities may be plasticizing the host. After an initial rapid decay to 60%, DCM slowly decays to 40% after 200 hours at 125° C. DADC is more stable retaining 75% of its original electro-optic coefficient after 200 hours at 125° C.

3. Three-Layer Slab Waveguides

Nonlinear optical materials must be formed into channel, slab, or rib waveguides for integrated optical applications. The resistance of crosslinked Ultradel 9020D to organic solvents

makes it a suitable material for layered devices. We formed three-layer slab waveguides by spinning and curing successive layers of Ultradel 9020D on ITO-coated glass. The layered structures consisted of DCM- and DADC-doped Ultradel 9020D cores surrounded by neat Ultradel 9020D cladding layers. To obtain noncentrosymmetric ordering as well as large poling field induced nonlinearities in three-layered devices, it is essential for the cladding layers to be more conductive than the core layer so that the voltage drop, and hence the poling field, across the active layer is as large as possible. Direct measurements of the poling field are not possible in three-layer samples because the voltage splitting between core and cladding layers is unknown. The effective poling field can be determined indirectly by measuring the macroscopic susceptibility's dependence on the externally applied field and comparing to theory. The macroscopic susceptibility was measured using the Rotational Maker Fringe (RMF) technique as a function of poling field for single- and three-layer samples.[32] Gold electrodes were sputtered onto the samples for contact poling. After contact poling, the gold was removed and the RMF experiment was performed. Measurements were made using the 2nd Stokes line ($\lambda = 1.367\mu$) of a hydrogen-filled Raman cell that was pumped by the output of a Nd:YAG pumped pulsed dye laser. For single-layers the poling field-induced nonlinearity is described by,

$$d_{33} = N f^{2\omega'} f^{\omega'} f^{\omega'} f^{o} \beta_{zzz} \frac{\mu E_p}{5 k_B T_p} \tag{3}$$

which relates the macroscopic susceptibility to microscopic parameters.[32] Fig. 11 shows the results for DCM and DADC single-layer samples. The solid line represents the predicted value for the nonlinear optical susceptibility, d_{33}, which includes the microscopic parameters obtained from EFISH experiments and the data points from RMF measurements. The agreement between theory and experiment shows that the oriented gas model adequately describes the poling induced ordering in polyimide materials.

The data for three-layer samples appear in Figs. 12a and 12b for DCM- and DADC-doped samples, respectively. The two sets of data points on the graphs represent different methods of calculating the poling field across the active layer. The open data points assume the resistivities of all three layers are identical and the resulting poling field is obtained by dividing the applied voltage by the total thickness. The shaded data points use a scaling factor to fit the experimental data to the theoretical prediction of Eq. 3 with the poling field as an adjustable parameter. If we assume the three-layer sample can be modeled by resistors in series, then the scaling factor can be related to the cladding and core resistances by the following equation,

$$V_{eff} = \frac{R_{core}}{R_{core} + 2R_{cladding}} V_{applied} \tag{4}$$

where R_{core} and $R_{cladding}$ are the resistances of the core and cladding layers, and V_{eff} and $V_{applied}$ are the effective and applied poling voltages.[33] The open data points show the inadequacy of assuming equal resistivities to determine the poling field across the active layer. For DCM triple-layers, a value of 0.4 is used for the best fit adjustable parameter, while for DADC triple-layers, a value of 0.11 is obtained. Conductivity of thin single-layer films was used to independently calculate the effective poling field. Conductivity measured as a function of temperature for DCM/Ultradel 9020D, DADC/Ultradel 9020D, and Ultradel

9020D is shown in Fig. 13. The conductivity and thickness of DADC triple-layers poled at 250° C predicts a correction factor of 0.1 in excellent agreement with the best fit. Thus, the voltage division model appears valid. For DCM triple-layers poled at 225° C Eq. 4 predicts an effective poling field an order of magnitude smaller than the best fit adjustable parameter. This discrepancy may be due to migration of DCM into the cladding layers which lowers the conductivity of the core layer while increasing the conductivity of the cladding layers. This migration is consistent with the sublimation observed in single-layer films. The optimization of poling requires that the conductivity of the cladding be much larger than the core to maximize the electric field in the active layer. Finding methods to adjust conductivity are important. We have found that the conductivity of polymer compositions can be controlled by adjusting the degree of fluorination of the polymer.

4. Channel Device Fabrication

A processing scheme for creating channel devices has been developed. This process is shown in Fig. 14. The photosensitive polymer is spin-deposited onto a substrate, and soft-cured (below $200°C$) to remove solvent. The polymer is exposed through a photomask leading to photo-crosslinking, and then partially etched with organic solvent developers into a rib or channel pattern. The coating is then post-baked at $300 - 350°C$ to remove residual solvent and to fully crosslink. Either rib or channel waveguides can be produced with this method.

Fig. 15 shows a SEM micrograph of a rib structure fabricated using photosensitive polyimides showing their high quality structure. Channels and ribs 4-5 microns wide have been produced. After post-cure, the films can withstand processes such as metallization, overcoating, thermal cycling, and solvent exposure. Waveguide loss spectroscopy was carried out on three-layer rib waveguides composed of two variations of Ultradel 9020D polymers with appropriate refractive indices. No excess optical loss was introduced by channel waveguide fabrication.

5. Conclusions

We have described the development of a crosslinkable polyimide material system for integrated optical applications. First, we optimized the optical and waveguide processing properties, and later introduced functionality by guest-host inclusion and electric field poling. From optical waveguide and PDS measurements we determined the primary mechanism for optical waveguide loss in polyimide waveguides is absorption from electronic absorption tails. The measured waveguide loss in Ultradel 9020D of 0.4 dB/cm at 800 nm and predicted losses of 0.3 dB/cm at 1300 nm make these materials excellent candidates for integrated optical applications. Introduction of the active chromophores, DCM and DADC, increased the optical losses as determined by PDS. We believe that these long absorption tails may be a general problem in the realization of electro-optic polymers.

We then studied the electric field poling conditions. The optimum poling temperature was found to be slightly below the sublimation temperature of DCM and well below the thermal decomposition temperature of most thermally stable chromophores. Both guest-host systems display excellent thermal stability of the electric field-induced orientation at

room temperature. At elevated temperatures, significant orientational relaxation occurred in DCM-doped samples. The enhanced decay may be attributed to plasticizing of the polyimide and greater rotational mobility of DCM. The DADC-doped polyimide retained 75% of its initial orientation after 200 hours at 125^0 C.

Three-layer samples of doped polyimide showed nonlinearities smaller than comparable single-layer films. The decrease in nonlinearity is attributed to lower poling fields due to voltage division across the three-layer sample and possibly chromophore migration into cladding regions. The voltage splitting can be eliminated by substituting existing cladding layers with more conductive cladding layers.

We have also described a simple waveguide processing procedure for forming channel and rib structures which takes advantage of the photocrosslinking nature of polyimide materials and does not introduce excess optical losses. We believe that this material system is an excellent candidate for active and passive integrated optical applications. Further refinement in processing and refractive index control are all that is necessary for passive applications. For active applications, the identification of suitable chromophores which do not introduce absorption is necessary. Covalent attachment of active chromophores to crosslinking sites should be straightforward, and would lead to vastly improved performance regarding optical nonlinearity and stability.

6. Acknowledgements

This work was performed, in part, at Sandia National Laboratories and was supported by the U.S. Department of Energy under contract DE-AC04-94AL85000. Partial support for this work was provided by AFOSR under grant # 49620-93-1-0202. The authors wish to thank S. Ermer (Lockheed)for chromophore synthesis and C. Allen (Amoco) for her technical assistance.

Literature Cited

1. G.I. Stegeman and W. Torruellas, MRS Proc., A.F. Garito, A. Jen, C. Lee, and L.R. Dalton, ed., Materials Research Society, Pittsburgh, **328**, 397 (1994).
2. P.M. Ranon, Y. Shi, H Steier, C. Xu, B. Wu, L.R. Dalton, Appl. Phys. Lett. **62**, 2605 (1993).
3. W. Sotoyama, S. Tatsuura, and T. Yoshimura, Appl. Phys. Lett. **64**, 2197 (1994).
4. B. Wu, C. Xu, L.R. Dalton, S. Kalluri, Y. Shi, and W. H. Steier, in MRS Proc., A.F. Garito, A. Jen, C. Lee, and L.R. Dalton, ed., Materials Research Society, Pittsburgh, **328**, 529 (1994).
5. J.W. Wu, J.F. Valley, S. Ermer, E.S. Binkley, J.T. Kenney, G.F. Lipscomb, and R. Lytel, Appl. Phys. Lett. **58**, 225 (1991).
6. J.W. Wu, E.S. Binkley, J.T. Kenney, R. Lytel, and A.F. Garito, J. Appl. Phys. **69**, 7366 (1991).
7. J.F. Valley, J.W. Wu, S. Ermer, M. Stiller, E.S. Binkley, J.T. Kenney, G.F. Lipscomb, and R. Lytel, Appl. Phys. Lett. **60**, 160 (1992).
8. H.H. Fujimoto, S. Das, J.F. Valley, M. Stiller, L. Dries, D. Girton, T. Van Eck, S. Ermer, E.S. Binkley, J.C. Nurse, and J.T. Kenney, in MRS Proc., A.F. Garito, A. Jen, C. Lee, and L.R. Dalton, ed., Materials Research Society, Pittsburgh, **328**, 553 (1994).

9. J.W. Wu, J.F. Valley, S. Ermer, E.S. Binkley, J.T. Kenney, and R. Lytel, Appl. Phys. Lett. **59**, 2213 (1991).
10. S.F. Hubbard, K.D. Singer, F. Li, S.Z.D. Cheng, and F.W. Harris, Appl. Phys. Lett. **65**, 265 (1994).
11. K.Y. Wong and A.K.Y. Jen, J. Appl. Phys. **75**, 3308 (1994).
12. B. Zysset, M. Ahlheim, M. Stahelin, F. Lehr, P. Pretre, P. Kaatz, and P. Gunter, Proc. SPIE **2025**, 70 (1993).
13. W. Sotoyama, S. Tatsuura, and T. Yoshimura, Appl. Phys. Lett. **64**, 2197 (1994).
14. D. Yu, A. Gharavi, and L. Yu, Appl. Phys. Lett. **66**, 1050 (1995).
15. T. Kaino in *Polymers for Lightwave and Integrated Optics*, L. A. Hornak, ed., Marcel Dekker, New York, 1 (1992).
16. T.P. Russel, H. Gugger, and J.D. Swalen, J. Polym. Phys. **21**, 1745 (1983).
17. H. Franke in *Polymers for Lightwave and Integrated Optics*, L. A. Hornak, ed., Marcel Dekker, New York, 207 (1992).
18. R. Reuter, H. Franke, and C. Feger, Appl. Optics **27**, 4565 (1988).
19. J.M. Salley, T. Miwa, and C.W. Frank, Proc. MRS **227**, 117 (1991).
20. R.A. Norwood, D.R. Holcomb, and F.F. So, Nonlinear Optics **6**, 193 (1993).
21. A. Skumanich, M. Jurich, and J.D. Swalen, Appl. Phys. Lett. **62**, 446 (1993).
22. A.C. Boccara, D. Fournier, and J. Badoz, Appl. Phys. Lett. **20**, 1333 (1981).
23. A.J. Beuhler, D.A. Wargowski, T.C. Kowalczyk, K.D. Singer, Proc. SPIE **1849**, 92 (1993).
24. A.J. Beuhler and D. A. Wargowski, "Photodefinable Optical Waveguides", U.S. Patent No. 5,317,082 (May, 1994)
25. C.C. Teng, M.A. Mortazavi, and G.K. Boudoughian, Appl. Phys. Lett. **66**, 667 (1995).
26. S. Ermer, J.F. Valley, R. Lytel, G.F. Lipscomb, T.E. Van Eck, D.G. Girton, D.S. Leung, and S.M. Lovejoy, Proc. SPIE **1853**, 183 (1993).
27. S. Ermer, J.F. Valley, R. Lytel, G.F. Lipscomb, T.E. Van Eck, and D.G. Girton, Appl. Phys. Lett. **61**, 2272 (1992).
28. S. Ermer, D. Leung, S. Lovejoy, J. Valley, and T.E. Van Eck, in *Organic Thin Films for Photonic Applications Technical Digest*, 1993 Vol. 17 (Optical Society of America, Washington, D.C., 1993) pp. 70-72.
29. T.C. Kowalczyk, T.Z. Kosc, K.D. Singer, P.A. Cahill, C.H. Seager, M.B. Meinhardt, A. Beuhler, and D.A. Wargowski, J. Appl. Phys. **76** 2505 (1994).
30. K.D. Singer, M.G. Kuzyk, W.R. Holland, J.E. Sohn, S.J. Lalama, R.B. Comizzoli, H.E. Katz, and M.L. Schilling, Appl. Phys. Lett. **53**, 1800 (1988).
31. K.D. Singer, M.G. Kuzyk, and J.E. Sohn, J. Opt. Soc. Am. B **4**, 968 (1987).
32. K.D. Singer, J.E. Sohn, S.J. Lalama, Appl. Phys. Lett. **49**, 248 (1986).
33. H.C. Ling, W.R. Holland, and H.M. Gordon, J. Appl. Phys. **70** , 6669 (1991).

DISCLAIMER

This report was prepared as an account of work sponsored by an agency of the United States Government. Neither the United States Government nor any agency thereof, nor any of their employees, makes any warranty, express or implied, or assumes any legal liability or responsibility for the accuracy, completeness, or usefulness of any information, apparatus, product, or process disclosed, or represents that its use would not infringe privately owned rights. Reference herein to any specific commercial product, process, or service by trade name, trademark, manufacturer, or otherwise does not necessarily constitute or imply its endorsement, recommendation, or favoring by the United States Government or any agency thereof. The views and opinions of authors expressed herein do not necessarily state or reflect those of the United States Government or any agency thereof.

FIGURES

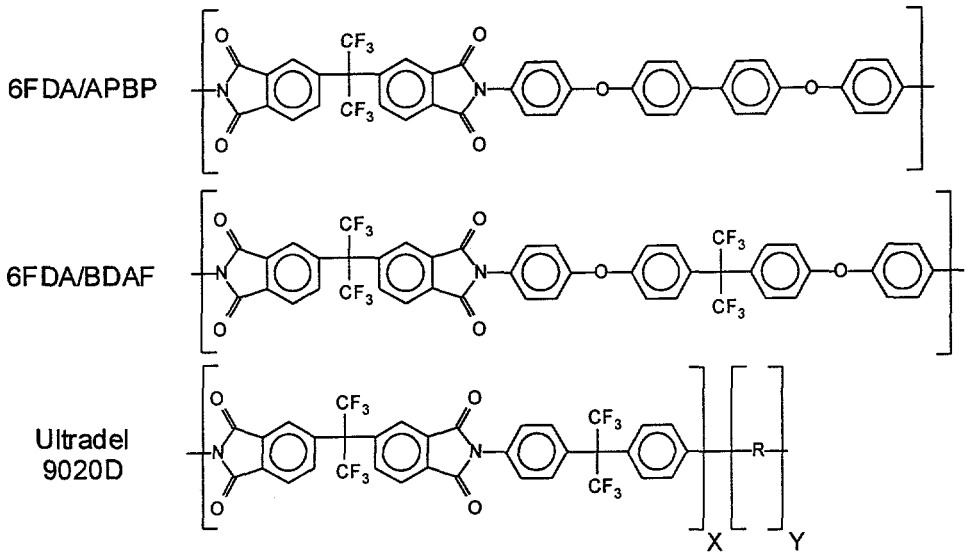

Fig. 1. Chemical structures of polyimides used in this study are listed in order of increasing fluorination. Ultradel 9020D is a crosslinkable polyimide. (R = alkylated aromatic crosslinking group as described in reference 24) Reproduced with permission from reference 29.

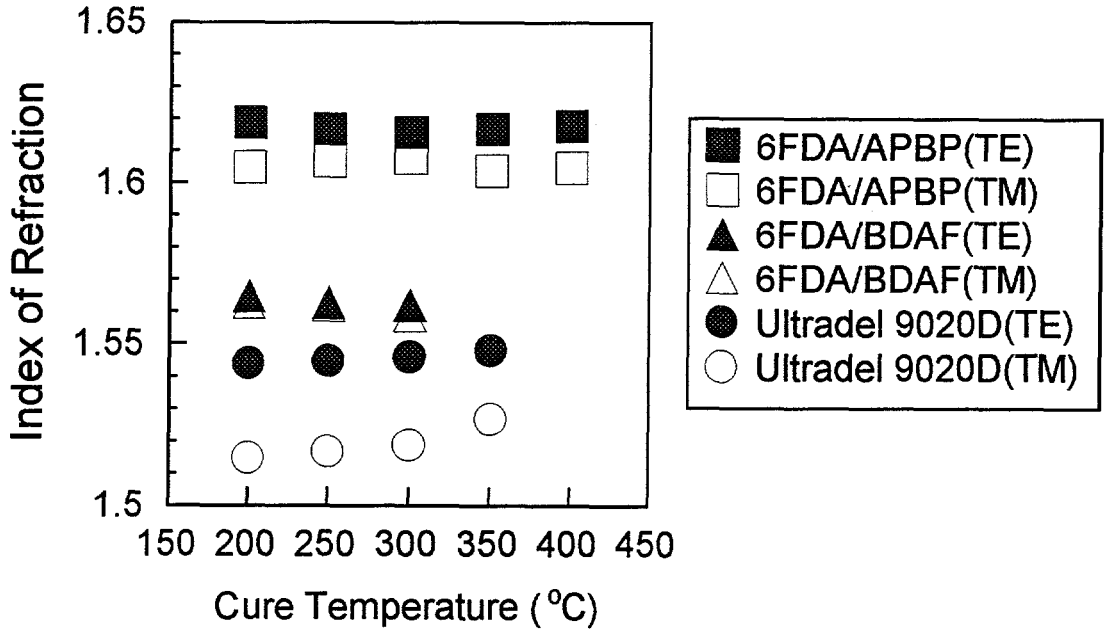

Fig. 2. TM and TE refractive index measurements at $\lambda = 632$ nm for polyimides shown in Fig. 1. Refractive indices and birefringences decrease with increasing fluorination. Reproduced with permission from reference 29.

Fig. 3. Comparison between PDS (lines) and WLS (data points). The losses decrease with increasing fluorination. The agreement between PDS and WLS suggests that losses are primarily absorptive. Reproduced with permission from reference 29.

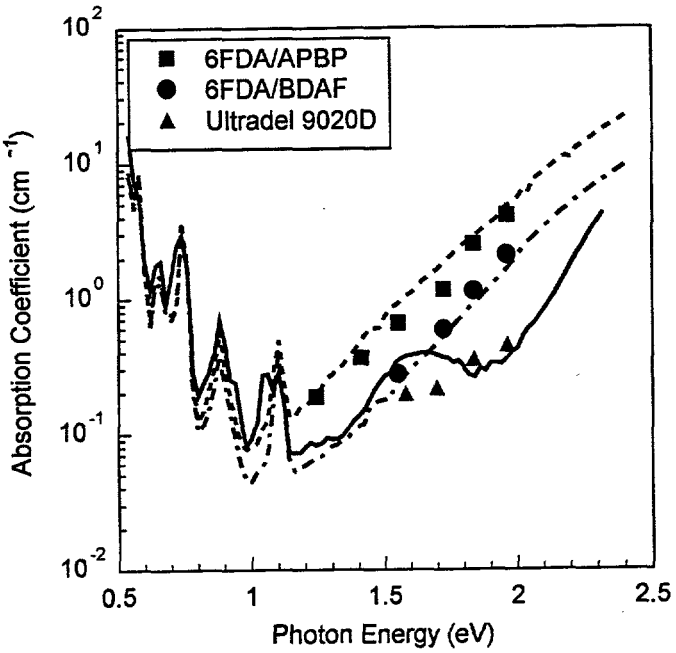

Fig. 4. WLS data at $\lambda = 800$ nm plotted as a function of curing temperature. Thermal crosslinking of Ultradel 9020D occurs near 200^{0}C. Processing variables significantly alter the optical properties of polyimides. Reproduced with permission from reference 29.

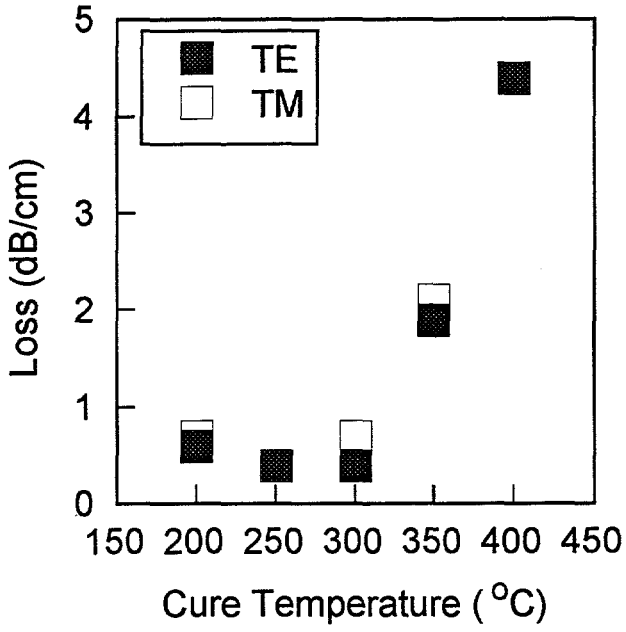

Fig. 5. Chemical structures and properties of thermally stable high temperature chromophores DADC and DCM.

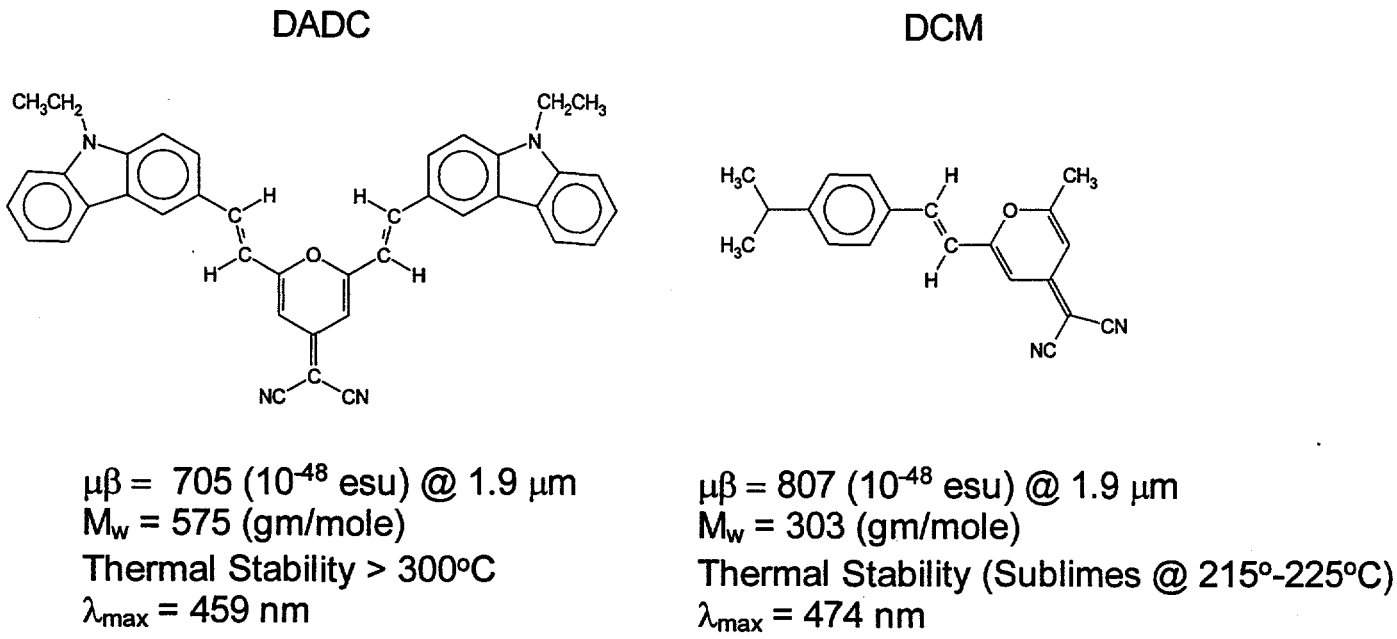

Fig. 6. PDS spectra showing the absorptive losses for Ultradel 9020D, DCM/Ultradel 9020D, and DADC/Ultradel 9020D. Chromophore loading is 17% by weight fraction. Curing temperatures for these samples were 300° C, 175° C, and 300° C, respectively.

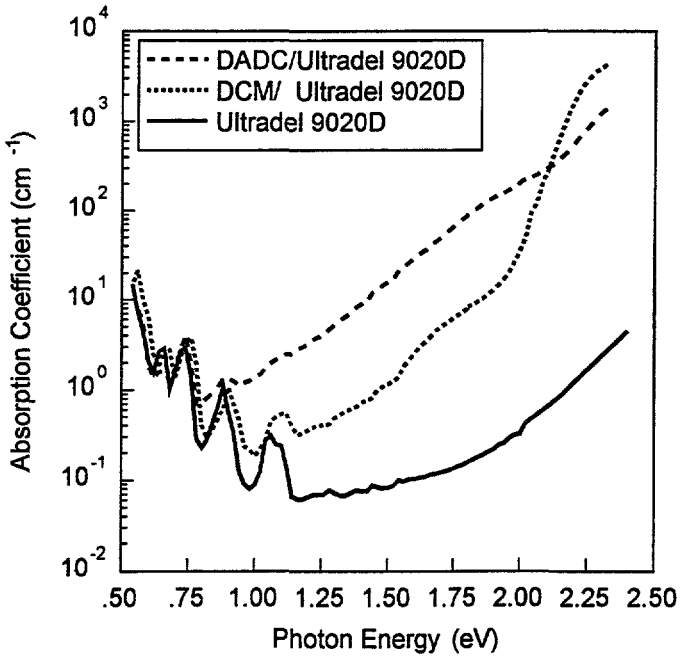

Fig. 7. Dielectric loss tangent of U9020D is plotted as a function of temperature for a sample processed at 175° C (dotted line). After cooling to room temperature the sample was remeasured (solid line). The solid line is multiplied by a factor of 100 to offset it from the dotted line for clarity.

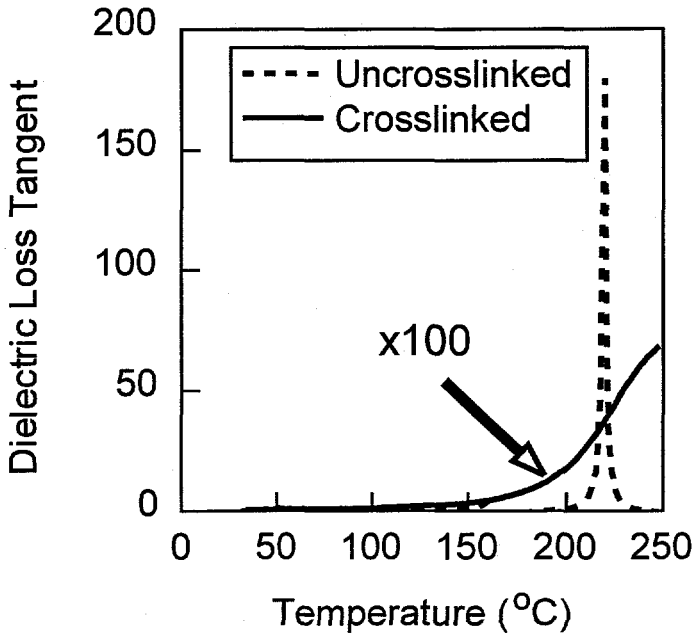

Fig. 8. Optical Absorption spectra of 20% DCM/U9020D at different curing temperatures. The inset shows the chromophore retention as measured by the change in optical absorption for samples of different initial weight fraction.

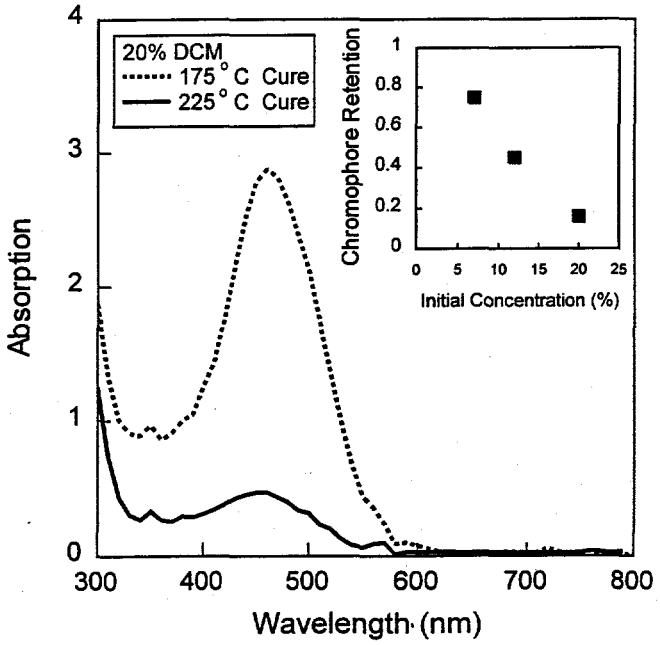

Fig. 9. Electric field dependence of electro-optic coefficient for 17% DADC by weight fraction. Solid lines represent (+/-)15% uncertainty in $\mu\beta$ values as input to the theory. Data points are from electro-optic experiment where $r_{33} = 3r_{13}$ was assumed.

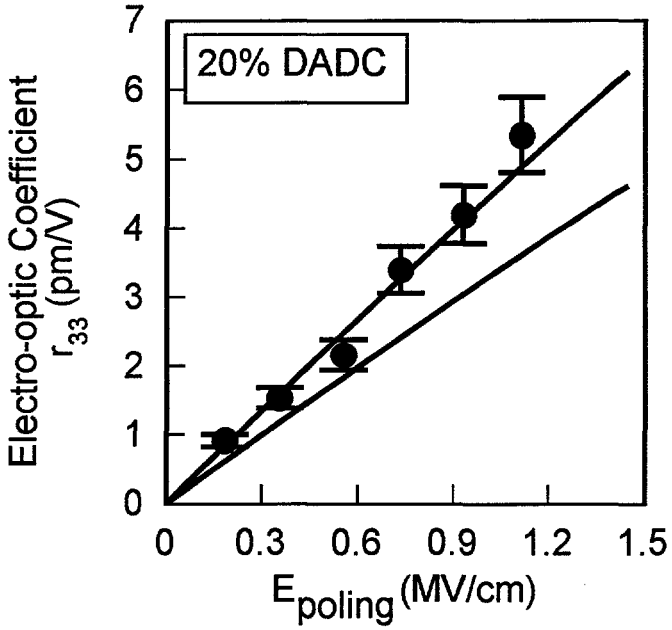

Fig. 10. Decay of electro-optic coefficient for DCM and DADC samples stored at 125° C. Electro-optic coefficients for DADC and DCM are normalized at $t = 0$.

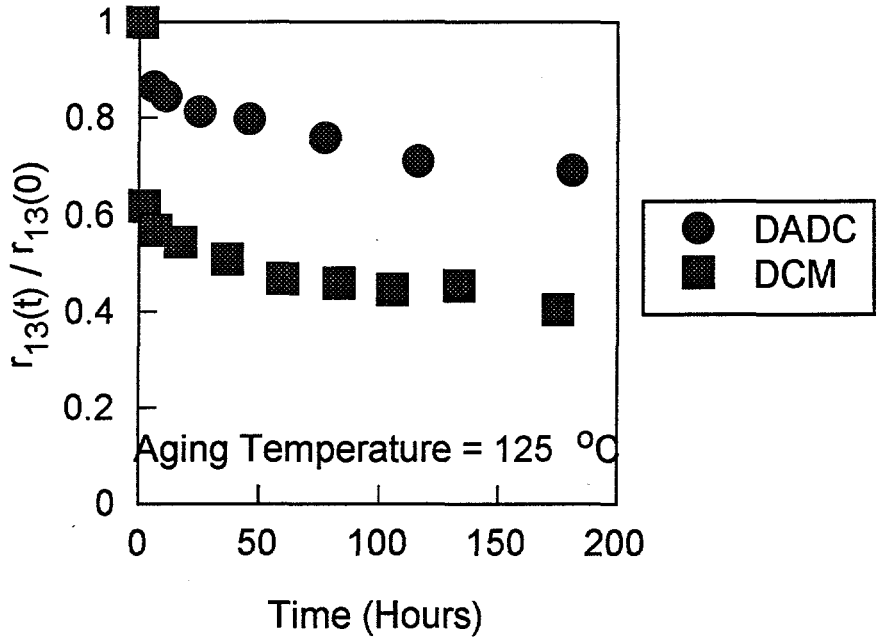

Fig. 11. d_{33} versus poling field for single layer DCM/Ultradel 9020D and DADC/Ultradel 9020D obtained from RMF experiments. Solid line represents calculation using Eq. 3 along with $\mu\beta$ values obtained from EFISH experiments. Agreement between theory and experiment shows the validity of using the oriented gas model to describe the poling process in guest-host polyimides.

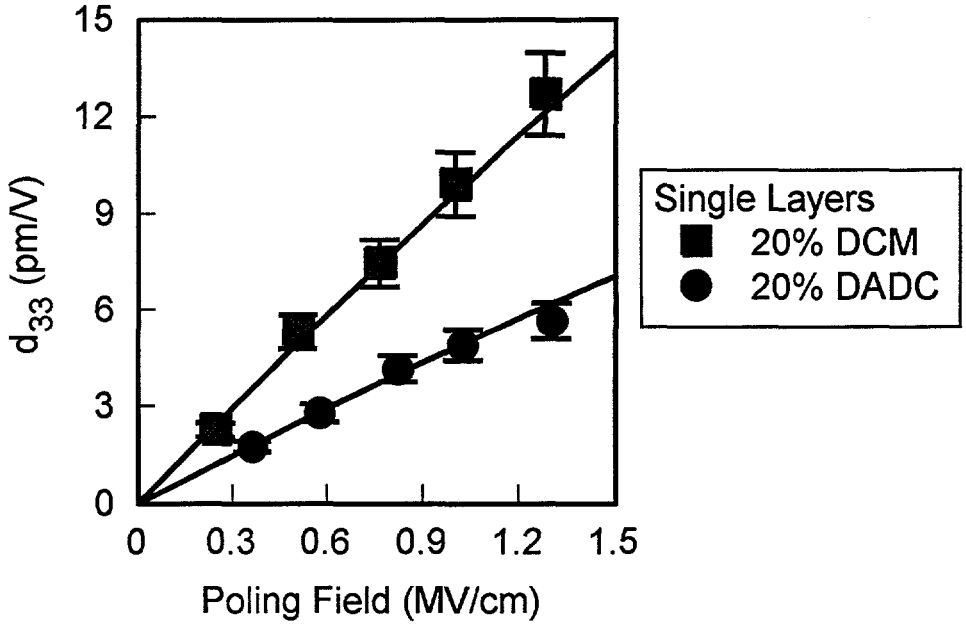

Fig. 12. d_{33} versus poling field for three layer stacks of (a) DCM/Ultradel 9020D and (b) DADC/Ultradel 9020D. Solid lines represents Eq. 3. Data points are measurements from three-layer samples using the poling field as an adjustable parameter. Best results (shaded data points) are obtained using 0.4 as the best fit parameter for DCM samples and 0.1 for DADC samples. (unshaded data points) assume that resistances of all layers are equal.

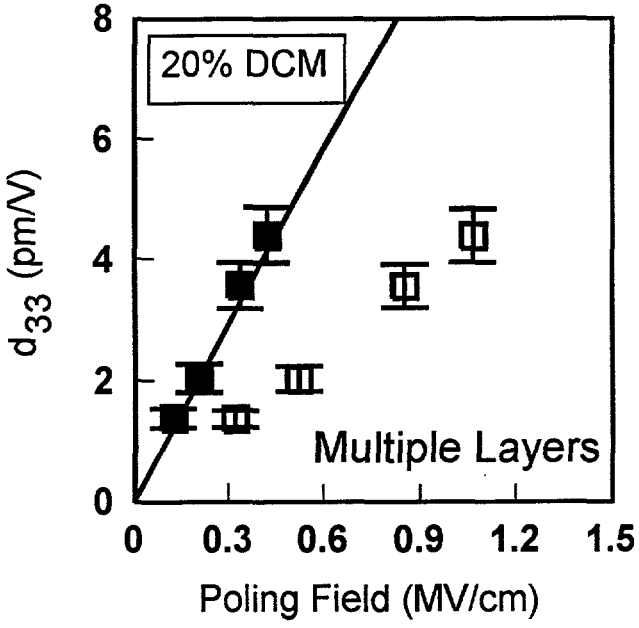

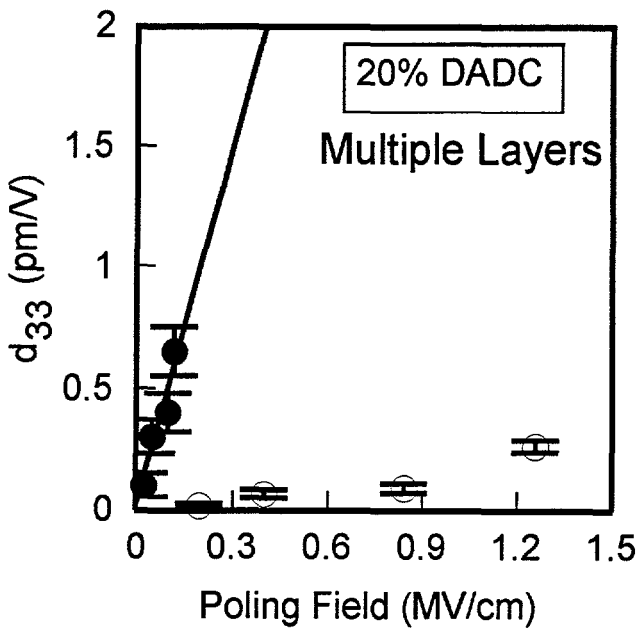

Fig. 13. Temperature dependent AC conductivity (0.1 Hz) for DCM/Ultradel 9020D, DADC/Ultradel 9020D, and neat Ultradel 9020D. An optimum three-layer stack would have cladding layers more conductive than the core.

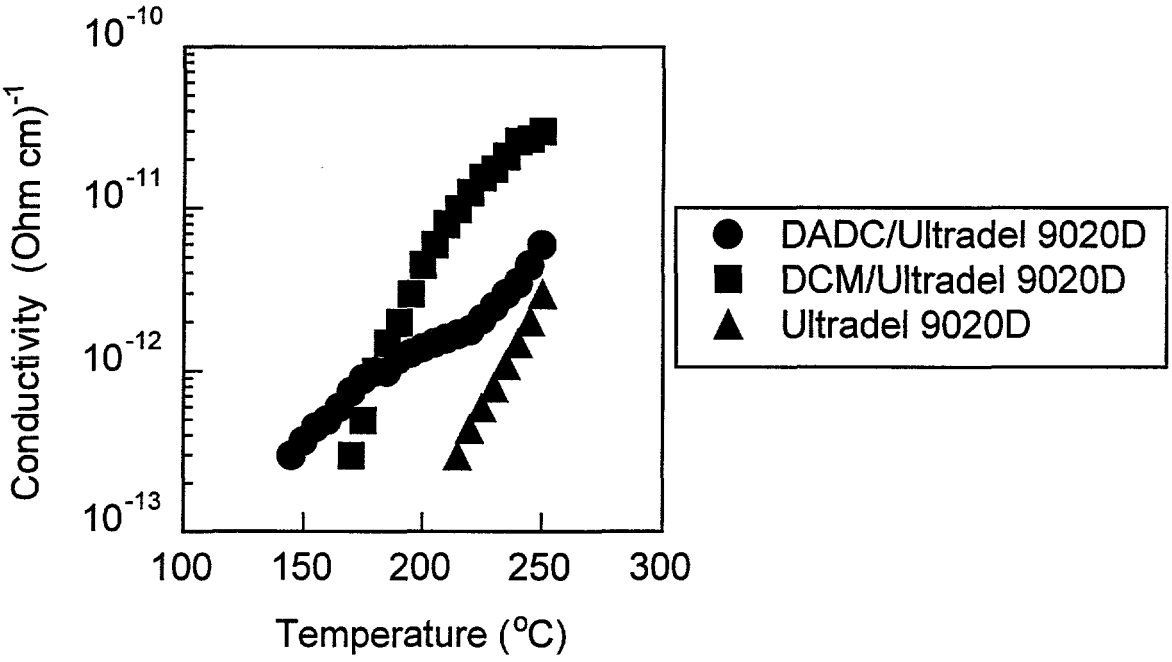

Fig. 14. Processing schematic for fabrication of single mode polyimide waveguides. Reproduced with permission from reference 23.

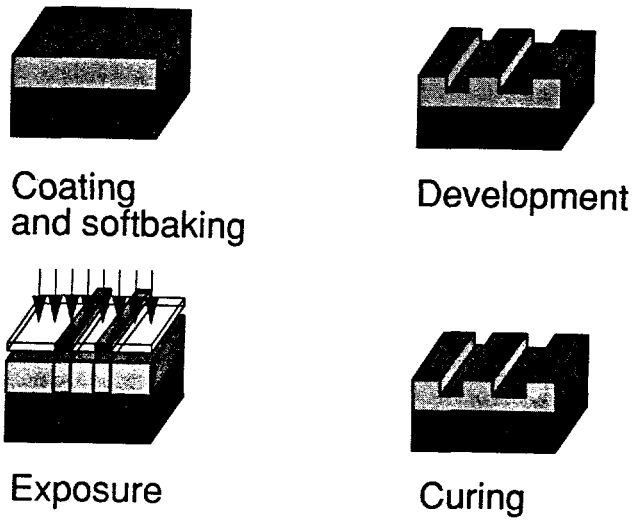

Fig. 15. SEM of 5.0 μm wide crossed rib waveguides etched in Ultradel 9020D.

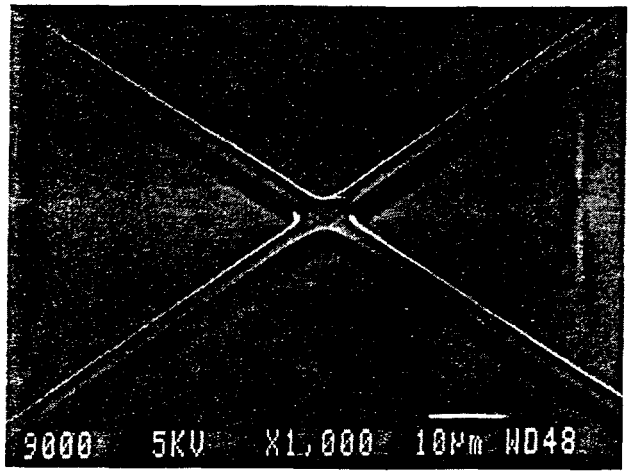

TABLES

	DCM/Ultradel 9020D				DADC/Ultradel 9020D		
$T_{poling}(^oC)$	175	195	215	235	175	225	275
$r_{33}(0)$(a.u.)	0.74	1.0	0.97	0.61	1.0	1.0	0.96
$r_{33}(t)$(a.u.)	0.23	0.49	0.48	0.27	0.58	0.96	0.92
$r_{33}(t)/r_{33}(0)$	0.31	0.49	0.49	0.44	0.58	0.96	0.96

Table 1. Dependence of electro-optic coefficient on poling temperature. Maximum electro-optic coefficient for DCM and DADC immediately after poling is scaled to unity for comparison purposes. Samples processed at temperatures above 200^o C have larger ratios.